Title

Active control of edge localized modes by radio frequency waves

Journal

Physics of Plasmas, 7(11)

ISSN

1070-664X

Authors

Avinash, K

Diamond, PH

Publication Date

2000-11-01

DOI

10.1063/1.1290050

Peer reviewed

Active control of edge localized modes by radio frequency waves

K. Avinash
Institute for Plasma Research, Gandhinagar 382428, India

P. H. Diamond
University of California, San Diego, La Jolla, California 92093-0319

(Received 25 February 2000; accepted 8 May 2000)

The effect of radio frequency wave driven torque on edge localized mode (ELM) activity is studied. It is shown that the radio frequency driven torque causes transition of type I giant ELMs to the benign grassy ELM behavior. The efficiency of this process scales directly with minor radius and inversely with the plasma density. It is argued that the technique of active ELM control will be efficient in the present for moderate-sized machines and in the future for large machines. © *2000 American Institute of Physics*. [S1070-664X(00)03410-8]

I. INTRODUCTION

The quasiperiodic oscillations in the tokamak edge during high-confinement mode (*H* mode), commonly called the edge localized modes (ELMs), are now routinely seen in all tokamaks under a variety of conditions and operating regimes. These oscillations have a beneficial effect on the confinement. During an ELM-free period, plasma density rises uncontrollably, often accompanied by impurity accumulation in the core. By periodically flushing these impurities, ELMs allow a steady state operation at constant-plasma density. Clearly, a successful advanced tokamak design aimed at steady state operation requires an ability to actively control and manipulate the ELM activity. Previously reported methods for influencing the ELM activity are varying separatrix to limiter[1] distance, controlling plasma shape, electron cyclotron resonance heating of the separatrix,[2,3] heavy gas fueling to cool the edge combined with off-axis heating by ion cyclotron resonance heating,[4] and the external magnetic perturbations.[5] Recently, efficient ELM control by varying the shape and the position of the plasma in the double null divertor configuration of the Tokamak Configuration Variable has been demonstrated.[6]

In this paper, we propose the injection of the ion Bernstein wave (IBW) for the control of ELM activity. In the Princeton High Beta Experiment (PBX),[7] the IBW was injected in a pre-existing high-confinement mode (*H* mode) to move the shear layer and the accompanying transport barrier from the edge to the plasma interior. The IBW resonance layer was placed in the plasma interior in this experiment. In this paper, we show that if the IBW can be absorbed efficiently near the edge, it can also provide an efficient method of ELM control. Specifically, we show that with a modest amount (~300 kW) of power, IBW driven torque lowers the critical energy flux $\bar{\Phi}_a$ for the onset of ELM activity. As a result, if the IBW is applied at low $\bar{\Phi}$ the ELM amplitude increases. At large power ($>\Phi_a$), however, the torque decreases the amplitude, increases the frequency, and thus causes a transition from type I giant ELM behavior to a benign ''grassy ELM behavior.'' The lowering of $\bar{\Phi}_a$ with the IBW is consistent with the recent observations on PBX[7] where an injection of IBW to an ELM free *H* mode caused a burst of ELM activity. Recent work by Craddock *et al*.[8] has shown that the IBW driven flows can lead to an effective suppression of fluctuations and improvement of confinement in the tokamak. The IBW driven torque has also been shown to be responsible for lowering *L* (low-confinement)→*H* transition threshold.

II. THE BASIC ELM MODEL

For the ELM activity, we invoke the recently proposed model of Lebedev *et al*.[9] In this model, it is shown that the ELM oscillations belong to the general category of relaxation oscillations. The ELM dynamics is determined by the interplay of a few basic processes at the plasma edge in the $L \rightarrow H$ transition dynamics, fueling of the edge by neutrals, and the evolution of the pressure gradient driven ideal ballooning mode fluctuations. In this basic model we incorporate the effect of the IBW driven poloidal flows.

We begin by describing briefly the salient features of the ELM model due to Lebedev *et al*. This model, which is spatially local, consists of four coupled equations for the normalized pressure gradient—p, the electric field shear U, the ambient background fluctuation due to ion temperature gradient or the drift wave (DW) ϵ_d, the magnetohydrodynamic (MHD) fluctuation level ϵ_m, and the poloidal velocity shear V. These equations are

$$\frac{\partial p}{\partial t} = \bar{\Phi} - p(d\epsilon_d + d_m\epsilon_m), \tag{1}$$

$$\frac{\partial V}{\partial t} = \epsilon_d U - (\bar{\mu} + \epsilon_m)V, \tag{2}$$

$$\frac{\partial \epsilon_m}{\partial t} = \bar{\lambda}(p-1)\epsilon_m, \tag{3}$$

$$\epsilon_d = p - U^2 \quad \text{if } p - U^2 > 0,$$
$$\epsilon_d = p - U^2 = 0 \quad \text{if } p - U^2 < 0, \tag{4}$$

$$U = V - \alpha p^2. \tag{5}$$

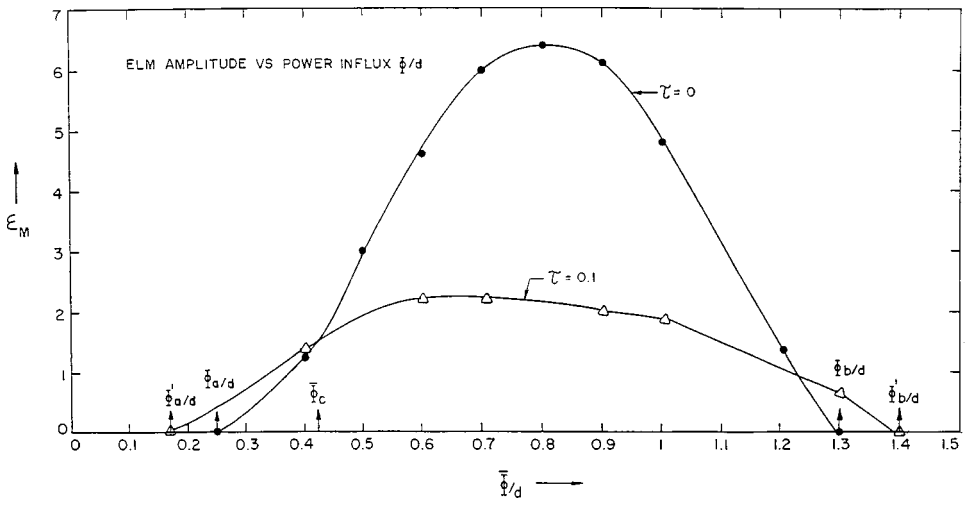

FIG. 1. Plot of ELM amplitude ϵ_m vs $\bar{\Phi}/d$ for $\tau=0$ and $\tau=0.1$. The other parameters are $\bar{\mu}=0.25$, $d=0.1$, $d_m=0.054$.

In this set, Eq. (1) describes the evolution of the pressure gradient under the influence of fueling by the particle flux $\bar{\Phi}$, the anomalous transport due to the ambient turbulence level ϵ_d, and the MHD fluctuation level ϵ_m. Since particle transport at the edge is mostly convective, $\bar{\Phi}$ is also proportional to the energy flux ($d\epsilon_d$ and $d_m\epsilon_m$ are respective diffusion coefficients). Equation (2) describes the generation of poloidal velocity shear due to Reynolds stress (the first term) and the damping due to magnetic pumping and MHD fluctuations. Equation (3) describes the evolution of the MHD fluctuations due to the pressure gradient drive with $p=1$ as the threshold in the appropriate normalized units. Equation (4) describes the ambient fluctuation level ϵ_d. These are excited by the pressure gradient drive and damped due to the nonlinear interaction and the electric field shear U, with $p-U^2=0$ as the threshold. It is assumed that the ϵ_d responds quickly to the changes in p and V so that $\partial\epsilon_d/\partial t=0$. The effect of rotation on evolution of ϵ_m is neglected for simplicity. Equation (5) describes the electric field shear due to the poloidal flow shear and the pressure gradient. The dimensionless constants d, d_m, μ, α, and λ are defined as

$$\bar{\lambda}=\sqrt{\frac{L_p}{R}}(\overline{k_\theta\rho_s})^{-1}\alpha_1/\alpha_3,$$

$$\bar{\Phi}=\frac{P_{\rm in}q^2}{\pi s r L_1 r_{\rm rec} c_s k_{\bar{\theta}}\rho_s B^2}\frac{\alpha_1}{\alpha_3}\left(\frac{Rq^2}{L_p s\beta}\right),$$

$$\bar{\mu}=\frac{\mu L_p}{c_s k_{\bar{\theta}}\rho_s}\frac{\alpha_1}{\alpha_3}\left(\frac{Rq^2}{L_p s\beta}\right), \tag{6}$$

$$d_m=\frac{L_p}{L_I},\quad d=\frac{\Delta_c^2}{L_p L_I}c_s\frac{\overline{k_\theta\rho_s}}{L_p\alpha_3}.$$

In these definitions μ is the magnetic pumping term. L_I and L_p are the penetration depth of neutrals and the width of the good confinement zone. Δ_c is the radial correlation length of DW fluctuations, c_s is the ion sound speed. s is the magnetic shear. R is the major radius, $r_{\rm rec}$ is the recycling rate, and q is the safety factor. Further, constants α_1, α_2, and α_3 depend on the specific turbulence model. The generic form of these constants is given in Refs. 10 and 11. The normalization of p, V, U, ϵ_d is also given in the same reference. It has been shown[10] earlier that if $\bar{\Phi}\geqslant\bar{\Phi}'$ ($\bar{\Phi}'$ is the threshold for $L\rightarrow H$ transition) then the radial E-field shear U is mainly due to poloidal flows. On the other hand, if $\bar{\Phi}>\bar{\Phi}'$, the E-field shear is mainly due to pressure gradients. The present discussion is limited to the regime $\bar{\Phi}\geqslant\bar{\Phi}'$ in which case $\alpha=0$ and $V\simeq U$. The typical values of the constants in Eqs. (1)–(5) are $\bar{\lambda}=5$, $\bar{\Phi}\sim 0.01$–0.2, $d_m\leqslant 0.1$, $\bar{\mu}\leqslant 1$, and $d\leqslant 0.1$.

As shown earlier,[9] these equations are sufficient to describe the transition from the L to H mode and the onset of ELM activity. For $\bar{\Phi}/d<\bar{\mu}^2$, the stable stationary point of the set of equations (1)–(5) is $\epsilon_d=p$, $\epsilon_m=0$, $V=0$, $p=(\bar{\Phi}/d)^{1/2}$. This point describes the L mode. At $\bar{\Phi}/d=\bar{\mu}^2$ this point loses stability and the plasma goes to a second stable stationary point given by $\epsilon_d=\bar{\mu}$, $V=(p-\bar{\mu})^{1/2}$, $p=\bar{\Phi}/d\bar{\mu}$, $\epsilon_m=0$. This is an ELM free H mode which persists for $\bar{\mu}^2 d<\bar{\Phi}<d\bar{\mu}$. At $\bar{\Phi}=\bar{\Phi}_a=d\bar{\mu}$, this stable fixed point goes over to a stable limit cycle via a Hopf bifurcation. These oscillations belong to the general class of ''relaxation oscillations'' where the pressure gradient reaches the ideal ballooning threshold given by $p=1$. This causes large spikes of ϵ_m which can be identified with type I giant ELM modes. With increasing $\bar{\Phi}$ the ELM frequency increases until at $\bar{\Phi}=\bar{\Phi}_b$ an inverse bifurcation to a stable fixed point occurs. As the system approaches this point, the amplitude of ϵ_m decreases, while the duration of ELM becomes comparable to the interval between two of them. This can be identified with the grassy ELM behavior. In Fig. 1, we plot the amplitude of ϵ_m for $\bar{\Phi}_a<\bar{\Phi}<\bar{\Phi}_b$.

It should be noted that in actual experiments, with increasing heating power, the sequence of events is a bit more complicated. Just after the $L\rightarrow H$ transition, there is a dithering period followed by a type III ELM. The question of understanding and resolving differences between dithering and type III ELM still remains unanswered.

III. THE EFFECT OF EXTERNAL TORQUE

We now proceed to incorporate the effect of IBW driven torque in this model. Craddock *et al.*[8] have shown that the

dominant contribution to IBW driven torque comes from the convective nonlinearity ($\tilde{v}\cdot\nabla\tilde{v}$) ($\tilde{v}$ is the fluctuating velocity due to IBW). In the present discussion we retain this contribution.

The equation for poloidal velocity in the presence of torque can be written as

$$\frac{\partial V}{\partial t}=\epsilon_d U-(\upsilon+\epsilon_m)V+\tau, \tag{7}$$

where τ denotes the radial derivative of the IBW driven torque. The normalization of τ is

$$\tau=\sqrt{\frac{\alpha_2}{\gamma_0}}\frac{(\tilde{v}\cdot\nabla\tilde{v})'}{\gamma_0},$$

where the prime denotes the radial derivative, γ_0 denotes the linear growth of DW, and α_2 is given in Ref. 10. Recently, Newman *et al.*[11] have used Eqs. (1)–(5) with $\epsilon_m=0$ to study the effect of torque on $L\rightarrow H$ transition. Their conclusions are that (a) a finite torque smoothens the $L\rightarrow H$ transition, and (b) it resolves the threshold for $L\rightarrow H$ transition in proportion to $\tau^{2/3}$. In order to estimate the typical values of τ we relate it to the absorbed rf power. Since IBWs are short scale length fluctuations, we may invoke slab approximation (x,y,z), in which case $\tilde{v}_x$ and $\tilde{v}_y$ are[8]

$$\tilde{v}_x=\frac{ie}{m_i(\omega^2-\Omega_i^2)}(\omega\bar{E}_x+i\Omega_i\bar{E}_y)e^{(\mathbf{k}\cdot\mathbf{r}-\omega t)}, \tag{8}$$

$$\tilde{v}_y=\frac{ie}{m_i(\omega^2-\Omega_i^2)}(-i\Omega_i\bar{E}_x+\omega E_y)e^{(\mathbf{k}\cdot\mathbf{r}-\omega t)}, \tag{9}$$

where ω, k, and $\bar{E}$ are the frequency, wave number, and the fluctuating E field of IBW, $|e|$, m_i, and Ω_i are the electronic charge, ion mass, and cyclotron frequency, respectively. In Eqs. (8) and (9), ω is real while $\bar{k}$ is complex. Since IBW is mostly radially propagating $\bar{k}\simeq k_x\hat{x}$, $E_x\gg E_y$. The mean torque is given by

$$\langle\tilde{v}\cdot\nabla\tilde{v}\rangle_y=\tilde{v}_x ik_x\tilde{v}_y=\frac{k_x^3c^2}{B^2}\frac{\omega^2\Omega_i^2}{(\omega^2-\Omega_i^2)^2}|\tilde{\varphi}|^2e^{\delta_e k_x^R x/2}, \tag{10}$$

where $k_x^R=\mathrm{Re}\,k_x$, $\delta_e=(\omega/k_\parallel v_{the})^2+\nu_e/\omega$, v_{the} is the electron thermal velocity, and ν_e denotes the electron–ion collision frequency. On the other hand, the absorbed IBW power is given by

$$P_{\mathrm{abs}}\simeq\frac{aR}{4\pi k_x}\frac{\delta_e\omega_{pe}^2}{\omega}k_z^2|\tilde{\mu}|^2, \tag{11}$$

where ω_{pe} denotes the electron plasma frequency, a and R are the minor and major radii, while k_z is the z component of $\bar{k}$. Using Eq. (11) to eliminate $|\tilde{\varphi}|^2$ in terms of P_{abs} in Eq. (10), the dimensionless radial derivative of torque τ can be expressed as

$$\tau=\left[\frac{\pi}{\delta_e}(k'\Delta_c)^2\left(\frac{k_x\eta c^2}{\gamma_0}\right)^2\left(\frac{k_x}{k_z}\right)^2\frac{\omega}{\gamma_0}\right]\frac{a}{L_n}\frac{1}{A^2q^2}\frac{1}{d^2}\bar{P}_{\mathrm{abs}}, \tag{12}$$

where we have grouped all the fluctuation parameters (which are relatively independent of the type of machine) together. In Eq. (12), the absorbed power is normalized to the ohmic power R_pI^2 [I and R_p are the plasma current and resistance, respectively, η is the plasma resistivity, L_n is the equilibrium scale, k' and Δ_c are the wave number and the radial mode width of DW fluctuations, γ_0 is the linear growth rate of DW fluctuations, and $d^{-1}=(c/\omega_{pe}a)$ is the collisionless skin depth. A is the aspect ratio and q is the safety factor at the edge]. Typically, $k_x/k_z=10^2$, $k_x\eta c^2/\gamma_0\simeq10^{-2}$, $\omega/\gamma_0\simeq10$, $k'\Delta_e\sim0(1)$ and in the high temperature plasma where collisionless damping is more important $\delta_e=(\omega/k_zV_{the})^3\simeq0(1)$. The efficiency of this scheme can be expressed in terms of a dimensionless parameter $Q=\tau/\bar{P}_{\mathrm{abs}}$, which roughly measures the amount of poloidal flow induced per unit power absorbed. Thus

$$Q=K\frac{a}{L_n}\frac{1}{A^2q^2}\frac{1}{d^2}, \tag{13}$$

where K [which represents fluctuation-dependent parameters within braces in Eq. (12)] is typically $\simeq10^4$. The efficiency directly scales with the minor radius a and inversely with the aspect ratio A, edge safety factor q, and the plasma density. The adverse scaling with the density in large machines like the International Tokamak Experimental Reactor (ITER)[12] is partially mitigated by the direct dependence on the minor radius a. Thus, for ITER parameters with edge density $n\simeq10^{14}\,\mathrm{cm}^{-3}$, $A\sim3$, $q\sim3$. Q ranges from 0.1 to 1. For smaller machines it is expected to be comparable to unity (on account of low edge density). In rf injected machines, absorbed rf power is a good fraction of the ohmic power, i.e., $\bar{P}_{\mathrm{abs}}=0(1)$, so that typically τ ranges from 10^{-2} to 10^{-1}. In our model we have neglected the effect of rf power in pressure evolution equation [Eq. (1)]. The reason is that pressure evolution is governed mainly by particle source due to external neutral beam with power in the range of a few megawatts and hence is much stronger than the rf power.

IV. RESULTS AND DISCUSSION

One important feature of the IBW driven torque is that the direction of the radial E field is always inward. This is in contrast to the case of the Alfvén wave,[13] where the direction of the E field is controllable. We now study the effect of τ in the regime of the onset of ELM activity. In case $\tau=0$, the critical Φ for the onset of ELM activity is $\Phi_a=\bar{\mu}d$. This can be obtained by linearizing the set of equations (1)–(5) around the ELM free stable H-mode point mentioned earlier. Since τ is typically small, a simple perturbative treatment gives the new threshold as

$$\bar{\Phi}_a'=\bar{\mu}d[1-\tau(\bar{\mu}-\bar{\mu}^2/2)^{-1}]. \tag{14}$$

This result is valid for $\tau/\bar{\mu}<1$. Since $\tau>0$, the threshold is reduced. This is consistent with the recent observations on PBX where the injection of the IBW in an ELM free mode is found to give rise to a burst of giant ELMs. In Figs. 2 and 3, we show the ELM amplitude and the associated pressure gradient oscillation for two cases: (i) $\tau=0$ and (ii) $\tau=0.1$. In the absence of torque, the MHD activity consists of a type I giant ELM characterized by a large amplitude and the duration of the event much smaller than the time interval between

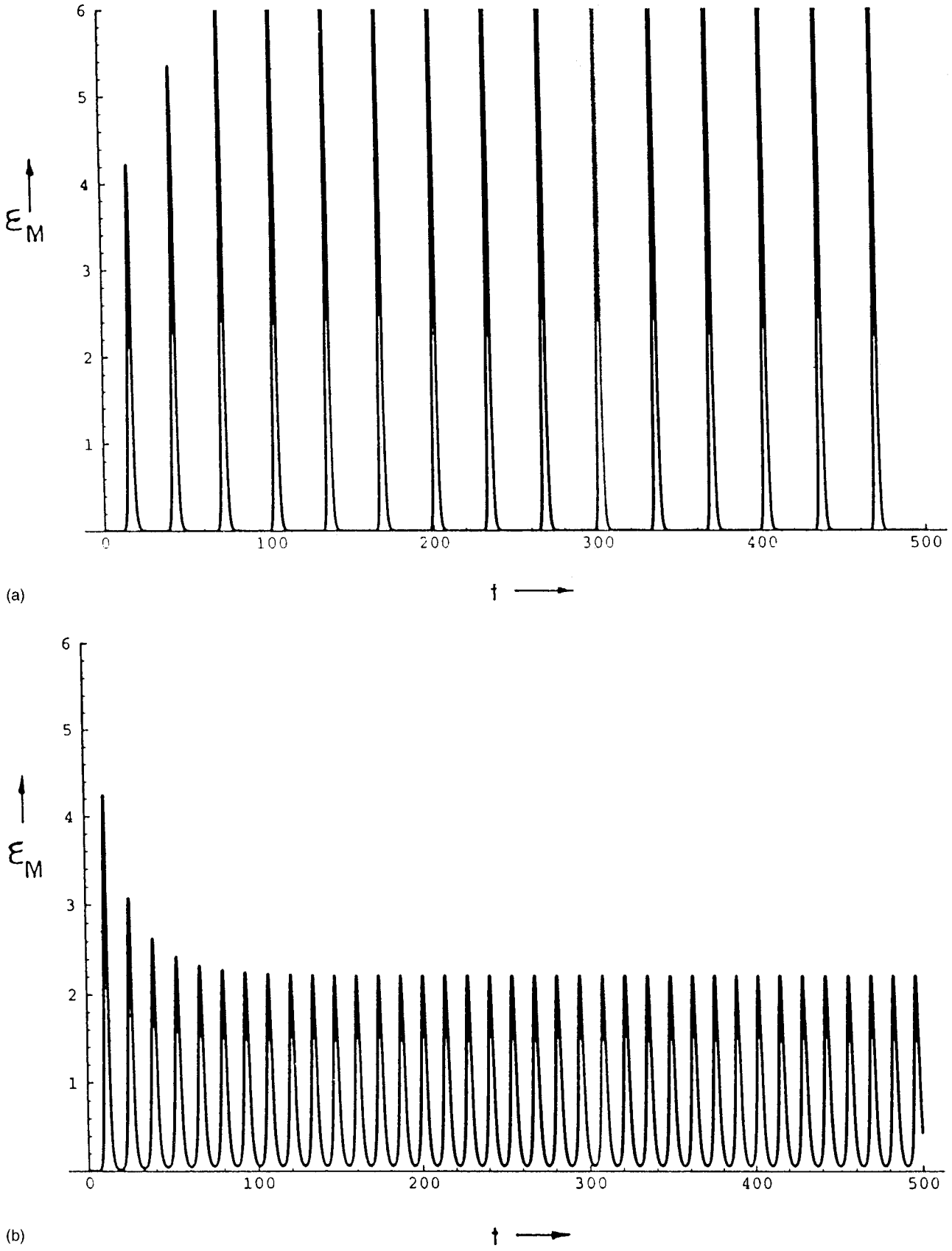

FIG. 2. ELM amplitude vs time for $\bar{\Phi}=0.09$, (a) $\tau=0$, (b) $\tau=0.1$. Other parameters are the same as in Fig. 1.

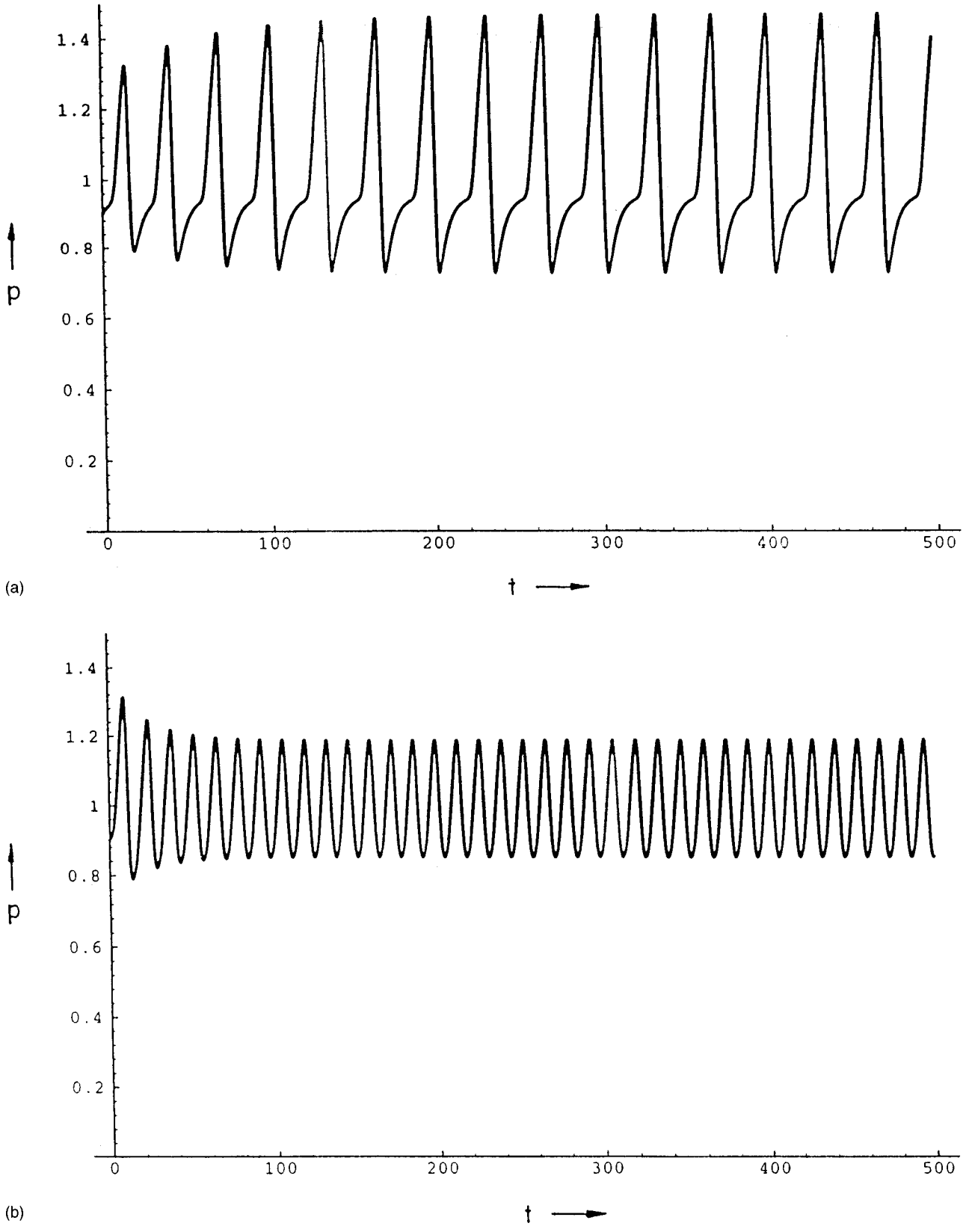

FIG. 3. Pressure gradient oscillations for $\bar{\Phi}=0.09$, (a) $\tau=0$, (b) $\tau=0.1$.

the two events. With the torque $\tau=0.1$, the amplitude of the ELM reduces by almost 300% while the frequency of events increases considerably. In this case, the duration of the event is comparable to the time interval between two events. This is the grassy ELM behavior. One notices similar trends in pressure gradient oscillations (Fig. 3). A finite torque thus causes a transition from type I to a benign grassy ELM behavior. In order to investigate the effect of external torque in

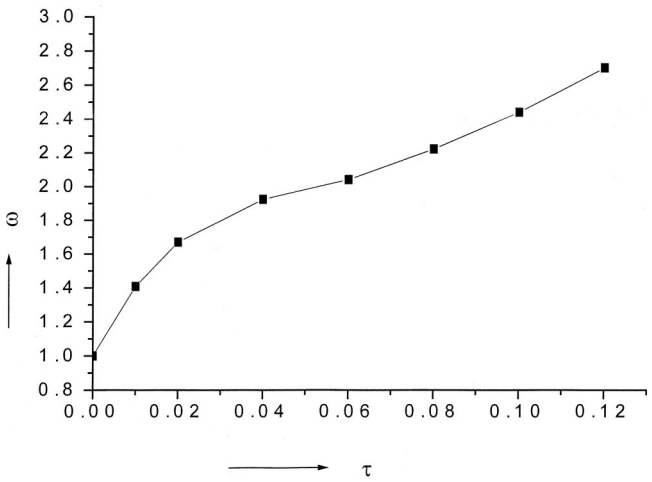

FIG. 4. Plot of ω vs τ. ω is defined as the ratio of frequency of the ELM without and with external torque τ. An increase of ELM frequency with τ is shown.

more detail we plot the ELM amplitude vs $\bar{\Phi}$ for the entire range $\bar{\Phi}'_a \leqslant \bar{\Phi} \leqslant \bar{\Phi}'_b$ in Fig. 1 where $\bar{\Phi}'_b$ is the threshold for inverse Hopf bifurcation to the stable fixed point. For $\tau=0.1$, $\bar{\mu}=0.25$, $d=0.1$, the value of $\bar{\Phi}'_a/d \simeq 0.15$ [from Eq. (14)], which is in rough agreement with the numerically calculated value of $\bar{\Phi}'_a/d=0.17$ shown in Fig. 1. Further, we notice that the effect of the external torque can be divided into three regimes of input power $\bar{\Phi}$. (i) For $\bar{\Phi}'_a \leqslant \Phi < \bar{\Phi}_c$, the external torque increases the amplitude of ELMs. (ii) For $\bar{\Phi} \simeq \bar{\Phi}_c$, the effect on ELM amplitude is weak. (iii) For $\bar{\Phi}_c < \Phi \leqslant \bar{\Phi}'_b$, the torque decreases the amplitude and causes a transition to grassy ELM behavior. In Fig. 4 we show this transition of giant ELMs to grassy ELMs by showing the increase of ELM frequency with the external torque. For $\tau=0.1$ the frequency of ELM is increased by a factor of 3. For PBX[7] parameters ($a=30\,\mathrm{cm}$, $n=2\times10^{13}\,\mathrm{cm}^{-3}$). $Q \simeq 2$, $\tau=0.1$, which corresponds to rf power $\simeq$300 kW. Thus the ELM activity in this model can be efficiently controlled. We have also studied the case with $\tau=10^{-2}$. In this range the effect is found to be very weak.

In Ref. 8 a high power regime, $\bar{\Phi} \gg d\bar{\mu}^2$ ($\bar{\Phi}=d\bar{\mu}^2$ is the threshold for $L \rightarrow H$ transition), has also been studied. This regime is characterized by an E field, which is mainly due to the pressure gradient and a strong damping of poloidal flows. Since external torque operates via poloidal flows (which are strongly damped) its effect on ELMs in this regime is expected to be weak. The physical reason for the transition of Giant ELMs to ''grassy'' ELM behavior is as follows. Clearly, any process which leads to a quick recovery of the transport barrier (thereby increasing the frequency of oscillation) will, in turn, lead to the reduction in amplitude. For instance, with the high beam power, on account of enhanced neutral beam fueling, the transport barrier recovers quickly and the amplitude is reduced. A somewhat similar mechanism operates in the present case. With rf driven torque the plasma spins faster, and as a result the DW saturtion level ϵ_d [Eq. (4)] is reduced. This leads to a reduction in the smearing of the barrier due to DW fluctuations [Eq. (1)]. As a result the barrier recovers quickly, causing a reduction in the amplitude and transition to the grassy ELM behavior.

Plasma heating via IBW has been performed on a number of experiments—Alcator C,[14] Princeton Large Torus,[15] Japanese Institute of Plasma Physics II—upgrade,[16] and PBX. In the last experiment, with a modest amount of rf power ($\sim$300 kW) a significant poloidal flow ($\sim 5 \times 10^4$ cm/s) and an inward E field was generated. However, the main objective of rf injection in this experiment was to move the shear layer in the plasma core. Hence the IBW resonance layer was located in the plasma interior. For efficient ELM control the rf power should be absorbed near the edge. The efficiency of this process depends on the efficiency of torque generation due to rf power, given by factor Q in Eq. (13). In small machines (of the size PBX), the torque generation is expected to be efficient. The efficiency degrades with increasing density, however, in large machines like ITER, the inverse scaling with n is partially mitigated due to the direct dependence on the minor radius. Hence the technique is expected to be efficient for large machines as well.

[1] F. Ryter, O. Gruber, K. Buchl *et al.*, *20th EPS Conference on Controlled Fusion and Plasma Physics, Lisbon, 1993*, edited by J. A. Costa Cabral, M. E. Manso, F. M. Serra, and F. C. Schuller (European Physical Society, Petit-Lancy, 1993), Vol. 17C, Part 1, I-23.
[2] T. C. Luce, R. A. James, A. N. Fyakhretdinov *et al.*, *13th International Conference on Plasma Physics and Controlled Nuclear Fusion Research, Washington DC, 1990* (IAEA, Vienna, 1992), Vol. I, 631 pp.
[3] T. Ozeki, M. S. Chu, L. L. Lao, T. S. Taylor, M. S. Chance, S. Kinoshita, K. H. Burrell, and R. D. Stambaugh, Nucl. Fusion **30**, 1425 (1996).
[4] P. R. Thomas, D. J. Campbell, A. Gondahalekar, and C. J. Lowry, *1992 International Conference on Plasma Physics, Innsbruck, 1992*, edited by W. Freysinger, K. Lackner, R. Schrittwieser, and W. Lindinger (European Physical Society, Petit-Lancy, 1993), Vol. 16C, Part I, 239 pp.
[5] T. N. Todd, ''Compass team,'' Plasma Phys. Controlled Fusion **B35**, 231 (1993).
[6] M. J. Dutch, F. Hofmann, B. P. Duval *et al.*, Nucl. Fusion **35**, 650 (1995).
[7] M. Ono, R. Bell, S. Bernabei *et al.*, *15th International Conference on Plasma Physics and Controlled Nuclear Fusion Research, Seville 1994* (IAEA, Vienna, 1995), Vol. I, p. 469.
[8] G. G. Craddock, P. H. Dimond, M. Ono, and H. Biglari, Phys. Plasmas **1**, 1944 (1994).
[9] V. B. Lebedev, P. H. Diamond, I. Gruzinova, and B. A. Carreras, Phys. Plasmas **2**, 3345 (1999).
[10] B. A. Carreras, D. Newman, P. H. Diamond, and Y. M. Liang, Phys. Plasmas **1**, 4014 (1994).
[11] D. E. Newman, B. A. Carreras, and P. H. Diamond, Phys. Plasmas **2**, 3044 (1995).
[12] R. Aymar, V. Chuyanov, M. Huguet *et al.*, *Fusion Energy, 16th Conference Proceedings, Montreal, 1996* (IAEA, Vienna, 1997), Vol. 1, p. 3.
[13] G. C. Craddock and P. H. Diamond, Phys. Rev. Lett. **67**, 1535 (1991).
[14] J. D. Moody, M. Porkolab, C. L. Fiore, F. S. Mcdermott, Y. Takase, J. Tery, and S. M. Wolfe, Phys. Rev. Lett. **60**, 298 (1988).
[15] M. Ono, P. Beisersdorfer, R. Bell *et al.*, *Proceedings of the 11th International Conference on Plasma Physics and Controlled Nuclear Fusion Research, 1986, Kyoto* (IAEA, Vienna, 1987), Vol. 1, p. 447.
[16] T. Seki, K. Kawahata, M. Ono *et al.*, *Ninth Topical Conference on Radio-frequency Power in Plasmas, Charleston, SC, 1991* (AIP, New York, 1991), p. 138.